

# AUTOMATIC EXTRACTION OF POWER LINES FROM MOBILE LASER SCANNING DATA

Haiyan Guan<sup>1</sup>, Jonathan Li<sup>2\*,1</sup>, Yongjun Zhou<sup>3,1</sup>, Yongtao Yu<sup>2</sup>, Cheng Wang<sup>2</sup>, and Chenglu Wen<sup>2</sup>

<sup>1</sup>Department of Geography and Environmental Management, University of Waterloo, Waterloo, Ontario N2L 3G1, Canada

<sup>2</sup>School of Information Science and Engineering, Xiamen University, Xiamen, Fujian 361005, China

<sup>3</sup>School of Naval Architecture, Ocean and Civil Engineering, Shanghai Jiaotong University, Shanghai 200240, China

Email: [h6guan@uwaterloo.ca](mailto:h6guan@uwaterloo.ca), [\\*junli@uwaterloo.ca](mailto:*junli@uwaterloo.ca), [allennessy.yu@gmail.com](mailto:allennessy.yu@gmail.com), [cwang@xmu.edu.cn](mailto:cwang@xmu.edu.cn),  
[mchapman@ryerson.ca](mailto:mchapman@ryerson.ca), [clwen@xmu.edu.cn](mailto:clwen@xmu.edu.cn)

## ABSTRACT

This paper presents a stepwise algorithm for extracting power-lines from mobile laser scanning (MLS) data. This algorithm first extracts non-road points from MLS data by estimating road ranges with regard to scanning mechanism and applying elevation-difference and slope criteria to the road ranges scan-line by scan-line. Then, three filters, in terms of height, spatial density, and size-and-shape, are proposed to extract power-line points in the identified non-road points, followed by Hough transform and Euclidean distance clustering. Finally, a 3D power line is modelled as a horizontal line in X-Y plane and a vertical catenary curve defined by a hyperbolic cosine function in X-Z plane. The proposed algorithm has been tested on a sample of point clouds acquired by a RIEGL VMX-450 MLS system. The results demonstrate the applicability of the proposed algorithm in extracting power transmission lines.

**Index Terms** – Mobile laser scanning, Point cloud, Power-line extraction, Euclidean distance clustering, power-line fitting

## 1. INTRODUCTION

As power lines interconnect various electrical power generation facilities and distributors of a bulk electricity transmission system, their safety significantly affects our daily lives and industrial activities. Accurately and timely monitoring power lines for re-engineering transmission lines and identifying possible encroachments is an extremely high priority for utility companies. At present, utility companies heavily rely on manual-operation methods, where many electrical linemen are hired to inspect, monitor, and maintain electrical distribution and overhead transmission lines. These methods are very time consuming and labor intensive. Aerial video surveillance or multispectral imaging is an alternative to overhead power line monitoring [1]. However, compared to field work, the image-based methods are

limited by the environmental conditions (e.g., light intensity, weather, and distracting background), stabilization of camera, and image degradation due to camera residual sightline motion [2-3]. Airborne laser scanning (ALS) systems have been gained popularity in documenting the majority of overhead transmission lines, in terms of high accuracy and high density [4-5].

Mobile Laser Scanning (MLS) system has become a promising means for land-based surveying and mapping since 2003 because MLS can produce extremely higher density point clouds, generating digital elevation models (DEMs) with the cm-level resolution, while most of ALS systems only have a 50 cm-level resolution. The excellent MLS data quality and accuracy allows users to determine various power-lines' physical parameters (e.g., catenary characteristics and vegetation encroachment distances) and use them for further engineering analysis [6-7].

In this paper, we propose a stepwise algorithm for directly extracting 3D power lines from MLS data. The algorithm detects curbs and separate non-road points from road points by estimating road ranges with regard to scanning mechanism and applying elevation-difference and slope criteria to MLS data scan-line by scan-line. Then, three filters (e.g., height, spatial-density, and size-and-shape) are proposed to isolate power-line points in the identified non-road points. Next, the extracted power-line points are grouped into a group of clusters representing individual power lines via Hough transform and Euclidean distance clustering. Finally, a 3D power line can be modelled as a horizontal line in X-Y plane and a vertical catenary curve defined by a hyperbolic cosine function in X-Z plane [8]. The proposed algorithm has been tested on a MLS dataset acquired by a RIEGL VMX-450 system.

## 2. MOBILE LASER SCANNING

MLS is opening new possibilities by enabling enormous of highly accurate, geo-referenced spatial data to be rapidly

collected and transformed into information-rich 3D infrastructure models. Most of MLS systems are composed of four key components: (1) laser scanners, (2) cameras, (3) a position and orientation system that integrates a Global Navigation Satellite System (GNSS) receiver, Inertial Measurement Unit (IMU) and a wheel-mounted Distance Measurement Indicator (DMI), and (4) a control system that synchronizes all sensors and manages data storages and communication.

The calculation of ground coordinates for illuminated objects is termed as “geo-referencing. The laser scanner is referenced when its position and orientation relative to the mapping coordinate system is known by a set of navigation system. These navigation data must be precisely time stamped for integration, and used to determine the exact locations of mapping points. The coordinates of a target  $P$  can be determined by

$$\begin{bmatrix} X_P \\ Y_P \\ Z_P \end{bmatrix}^M = \begin{bmatrix} X_{GPS} \\ Y_{GPS} \\ Z_{GPS} \end{bmatrix}^M + R_{IMU}^M(\omega, \phi, \kappa) \cdot \left( R_S^{IMU}(\Delta\omega, \Delta\phi, \Delta\kappa) \cdot r_p^S(\alpha, d) - \begin{bmatrix} L_X \\ L_Y \\ L_Z \end{bmatrix}_S^{IMU} \right) \quad (1)$$

where the parameters and their descriptions are listed in Table 1.

Table 1. Parameters of the geo-referenced equation

Parameters	Description
$X_P, Y_P, Z_P$	The location of the target P in the mapping frame.
$X_{GPS}, Y_{GPS}, Z_{GPS}$	The location of GPS antenna's phase centre in the mapping frame.
$r_p^S(\alpha, d)$	Relative position vector of Point P in the laser scanner coordinate system, $\alpha$ and $d$ are the scan angle and range measured and returned by the laser scanner.
$L_X, L_Y, L_Z$	The lever arm offsets from the navigation origin (IMU origin) to the measurement origin of the laser scanner. These values must be determined by system calibration or measurement.
$R_{IMU}^M(\omega, \phi, \kappa)$	Rotation matrix between IMU body frame and mapping frame, $(\omega, \phi, \kappa)$ are the roll, pitch and yaw of the sensor with respect to the local mapping frame. These values are determined by IMU.
$R_S^{IMU}(\Delta\omega, \Delta\phi, \Delta\kappa)$	Rotation matrix between the laser scanner and IMU, $(\Delta\omega, \Delta\phi, \Delta\kappa)$ are the boresight angles which align the scanner frame with IMU body frame. Those values must be determined by a system boresight calibration.

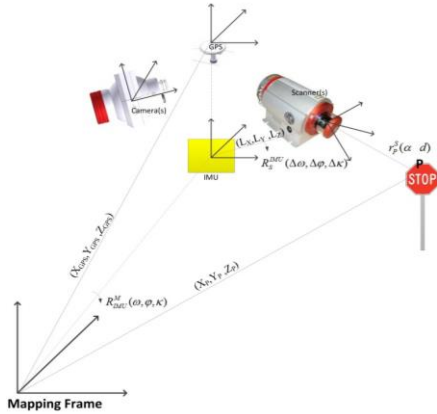


Fig. 1. Illustration of Geo-referencing.

### 3. METHODOLOGY

The proposed algorithm contains three steps: non-road point extraction, power-line extraction, and 3D power-line fitting.

#### 3.1. Non-road point extraction

Each laser scanner in the RIEGL VMX-450 system generates its own 360° “full circle” profile scans owing to the motorized mirror scanning mechanism. The scan angle ranges from -180° to +180°. The relation of the angular resolution to the ground distance for a given sensor elevation is formulated by:

$$\tan \alpha = D_h / h \quad (2)$$

where  $\alpha$  is the beam incidence angle,  $h$  is the sensor elevation from the ground, and  $D_h$  is the scanning distance between the scanner and the target of interest. In this study, the system configures two laser scanners at the angle of  $\eta = 45^\circ$  toward the rear of the vehicle, as shown in Fig. 2. The transverse range,  $D_t$ , from the point  $O$  to  $P$  is estimated by:

$$D_t = D_h \cos \eta \quad (3)$$

Thus, the relation of the incidence angle to the transverse range is represented by:

$$\tan \alpha = D_t / h \cos \eta \quad (4)$$

According to Eq. (4), a prior knowledge of road width is used to obtain point clouds in the incidence-angle range of  $[-K^\circ, K^\circ]$ .

Within the estimated angle extent of a road, we apply two criteria (i.e., elevation difference and slope) for curb extraction scan-line by scan-line. We mathematically define the slope between two consecutive points in a generated pseudo scan-line and the elevation difference of a point relative to its neighbourhood in the scan-line. First, slopes at the border of pavement and roadway are usually larger than those of continuous points on the roadway. Second, pavement points have larger elevations than road points in the neighbourhood. After identifying all curb corners from the scan-lines, a cubic spline interpolation is used to smooth the edges of the road and further extract non-road points

from MLS point clouds. The description of road extraction method can be found in [9].

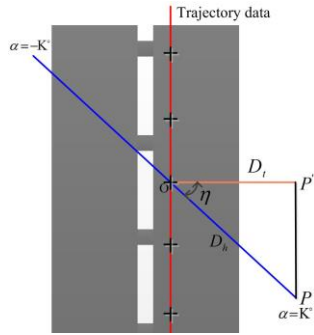


Fig.2. illustration of the relation of scan angle to scan distance.

### 3.2. Power-line extraction

Fig.3 shows the proposed power-line extraction method. As shown in Fig.3, three filters are used to extract power-lines from the identified non-road points; Hough transform and Euclidean cluster are further used to obtain individual power-lines.

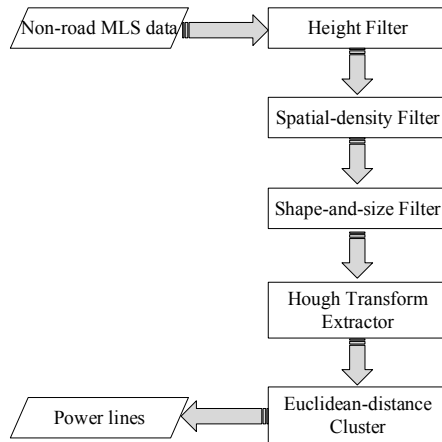


Fig.3. Flowchart of the proposed power-line extraction.

Every country has its own standards to the design and distribution of power lines with various types of voltage. For example, according to the National Electrical Safety Code (NESC), the vertical clearance to ground for power-lines of various voltages is exemplified as: 6.4 m (21ft.) for 138 kV, 7.0 m (23 ft.) for 230 kV, and 8.5 m (28 ft.) for 500 kV. Thus, a height filter is proposed to obtain power-line candidates.

After being filtered out large-scale terrain points and low-rise objects, besides power lines and towers, high-rise buildings and vegetation are still contained in the non-road point clouds. In addition, occlusions caused by high-rise buildings and other objects result in great challenges to the detection of power-lines and power-towers/poles along the corridor. Therefore, a spatial-density filter is proposed to further extract power-lines. Next, a shape-and-size filter is

used to remove other objects, such as trees, and preserve power-tower points in the spatial density map.

Hough transform is a common and efficient method in power-line extraction; thus, it is applied to the extracted power-line points. In order to group the classified power-line points into clusters representing separated power lines, a Euclidean distance clustering method is used to cluster the power lines with a pre-defined clustering distance. After applying the Euclidean distance clustering method, the classified power-line points are grouped to form individual power lines.

### 3.3. 3D Power-line fitting

In this section, a fitting methodology is proposed to project the 3D power-line points into the XY-plane and the vertical plane. In the XY-plane, the power lines can be described by a two-parametric model or a model with more than two parameters and additional constraints. It is given by the Hessian normal form:

$$x \cos \theta + y \sin \theta = \rho \quad (3)$$

where  $\theta$  and  $\rho$  are the angle of line's normal vector and X-axis, and the distance between the line and the origin, respectively. In the vertical plane, a catenary curve is fitted. A catenary curve  $C$  in the XZ-plane is given by:

$$z = a + c \cosh\left(\frac{x-b}{c}\right) \quad (4)$$

where  $a$  and  $b$  are the parameters for translation of the origin;  $c$  is a scaling factor denoted as the ratio between the tension and the weight of the hanging flexible wire per unit of length. The reconstruction of catenary curves is to find the optimal parameters (i.e.  $a$ ,  $b$ ,  $c$ ) via a group of the classified power-line points.

## 4. RESULTS AND CONCLUSION

We tested the proposed power-line extraction method on the MLS data acquired by a RIEGL VMX-450 system. The survey was conducted in a tropical urban environment, Xiamen, a port city in southeast China. Fig. 4 shows a road section of the collected MLS data. The proposed algorithm was applied to the selected dataset for the extraction of 3D power transmission lines.

In the non-road extraction, according to the prior knowledge of the investigated road section, the parameters used in this paper are empirically selected. The prior knowledge of the surveyed road section suggested  $D_h = 11.70$  m and  $\eta = 45^\circ$  and the range of incidence angles,  $K$ , is calculated at the range of  $-70^\circ$  to  $70^\circ$ . Within the calculated incidence-angle range, we kept the slope threshold of  $65^\circ$  and the elevation difference thresholds of 10-30 cm for detecting curb points scan-line by scan-line.

In the power-line extraction, The investigated areas in this study contain two types of power lines: (1) >138 kV voltage three-phase transmission lines across the road, and (2) 1-10 kV voltage transmission lines along the road. The power towers for the first type of transmission lines are larger than 30 m, while the power poles supporting the second type of transmission lines are ~ 6 m in height. Accordingly, the majority of low shrub hedges and trees are removed. A number of samples are selected to statistically obtain the threshold of spatial-density for extracting power-line points. The values of the size and shape thresholds, respectively, are 0.5 and 0.5 for the refinement of power-line points. Fig. 5 shows the extracted 3D power-line points.

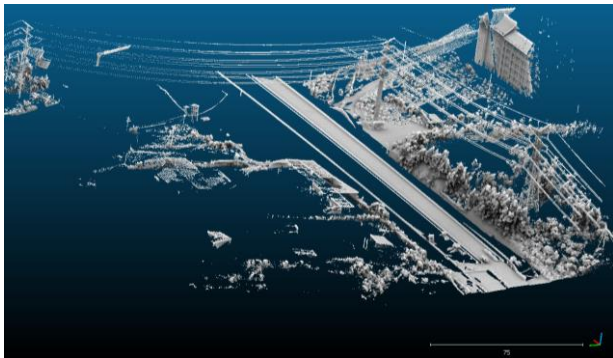


Fig.4. A road section of the collected RIEGL MLS data.

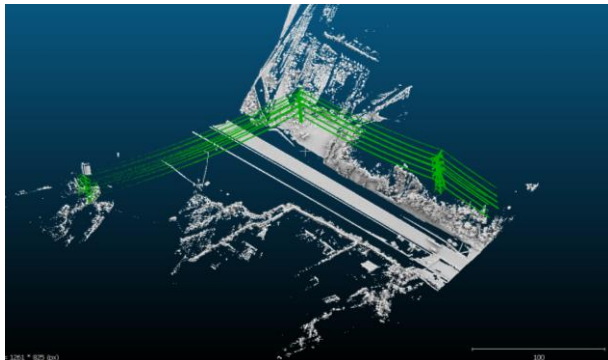


Fig. 5. Classified 3D power-lines and power-towers.

After the implementation of Hough transform, the extracted power-lines are clustered by a Euclidean cluster method with a certain size of cluster distance. In this study, the threshold of the cluster distance is 0.3 m because the vertical distances of power lines are less than 0.5 m. Fig. 6 shows the individual power-lines rendered by different colors.

All the extracted power-lines are fitted in XY planes and modelled in a 3D space. Fig. 7 shows the middle group of the power-lines modelled in a 3D space. The red points are the individual power-lines, and the blue lines are their fitted lines.

As seen from the extracted power lines and their fitted models, we conclude that the proposed step-wise algorithm performs very well and achieves reliable results.

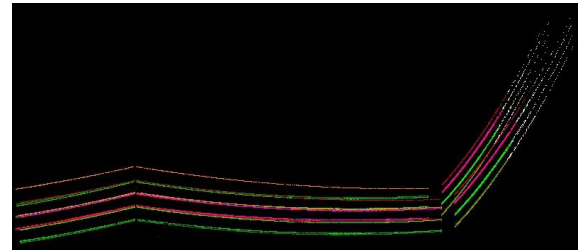


Fig. 6. Clustered 3D power lines.

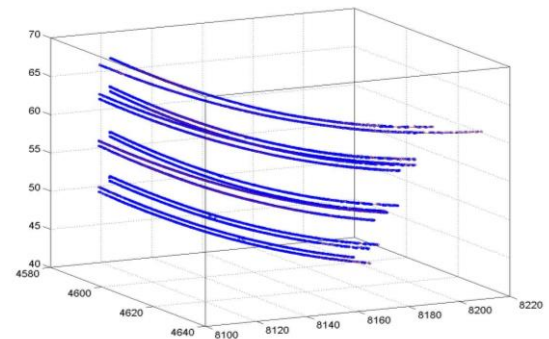


Fig. 7. A group of fitted catenary power lines in a 3D space.

## 5. REFERENCES

- [1] A. Junaid, A. S. Malik, L. Xia, and N. Ashikin, "Vegetation encroachment monitoring for transmission lines right-of-ways: A survey," *Electric Power Systems Research*, vol. 95, pp.339-352, 2013.
- [2] D.I. Jones, G.K. Earp, "Camera sightline pointing requirements for aerial inspection of overhead power lines," *Electric Power Systems Research*, vol. 57, pp. 73-82, 2001.
- [3] I. Golightly, D. Jones, "Corner detection and matching for visual tracking during power line inspection," *Image and Vision Computing*, 21, pp. 827-840, 2003.
- [4] Y. Jwa, G. Sohn, and H. B. Kim, "Automatic detection and modeling of powerline from airborne laser scanning data," *ISPRS Archives*, September 1-4, Paris, France, pp.105-110, 2009.
- [5] H. B. Kim and G. Sohn, "3D classification of power-line scene from airborne laser scanning data using random forests," *ISPRS Archives*, September 1-3, Saint-Mandé, France, vol. 38(3A), pp.126-132, 2010.
- [6] M. Lehtomäki, A. Jaakkola, J. Hyypä, A. Kukko, and H. Kaartinen, "Detection of vertical pole-like objects in a road environment using vehicle-based laser scanning data," *Remote Sensing*, 2(3), pp. 641-664, 2012.
- [7] A. Kukko, H. Kaartinen, J. Hyypä, and Y. Chen, "Multiplatform approach to mobile laser scanning," *ISPRS Archives* vol. 39 (B5), pp. 484-488, 25 August - 1 September 2012, Melbourne, Australia, 2012.
- [8] R.A. McLaughlin, "Extracting transmission lines from airborne LiDAR data," *IEEE Geoscience and Remote Sensing Letters*, vol. 3, no. 2, pp. 222-226, 2006.
- [9] H. Guan, J. Li, Y. Yu, C. Wang, M. Chapman, and B. Yang, "Using mobile laser scanning data for automated extraction of road markings", *ISPRS Journal of Photogrammetry and Remote Sensing* 87, pp.93-107,2014.